ELSEVIER

Journal of Alloys and Compounds 217 (1995) 226–234

Journal of ALLOYS AND COMPOUNDS

Absorption of hydrogen by palladium–nickel–rhodium ternary alloys

Y. Sakamoto [a], K. Ohira [a], N. Ishimaru [a], F.L. Chen [a], M. Kokubu [a], T.B. Flanagan [b]

[a] *Department of Materials Science and Engineering, Nagasaki University, Nagasaki 852, Japan*

[b] *Department of Chemistry, The University of Vermont, Burlington, VT 05405-0125, USA*

Received 30 June 1994

Abstract

The hydrogen absorption characteristics of Pd–Ni–Rh alloys ((1) $Pd_{97.5-x}Ni_{2.5}Rh_x$ with x (at.% Rh) = 0, 2.5, 5.0, 7.5, (2) $Pd_{95.0-x}Ni_{5.0}Rh_x$ with $x = 5.0$, (3) $Pd_{90.0-x}Ni_{10.0}Rh_x$ with $x = 7.5$, and (4) $Pd_{87.5-x}Ni_{12.5}Rh_x$ with $x = 2.5$, 5.0) have been investigated at temperatures between 273 K and 433 K and hydrogen pressures up to 1000 Torr, and for some alloys up to 10 000 Torr, by means of pressure–composition isotherm measurements, together with X-ray measurements of the lattice parameters of hydrogen-free and hydrogenated alloys. The dependence of the lattice parameters of the β_{min} phase boundaries of the hydrogenated low Ni content Pd–Ni–Rh alloys on the Rh content follows a similar trend to that exhibited by hydrogenated Pd–Rh alloys; these display an increase in the $a_{\beta_{min}}$ values with increasing Rh content up to about 7.5 at.% Rh. The low pressure solubilities of the ternary alloys decrease with Ni and Rh content, and the $\alpha+\beta$ plateau pressures increase. The hydrogen capacities of the Pd–Ni–Rh alloys with a given Ni content exhibit a maximum around 7.5 at.% Rh. The relative chemical potential $\Delta\mu_H^\circ$ of dissolved hydrogen at infinite dilution in the low Ni content Pd–Ni–Rh alloys increases with Rh content from that of Pd–Ni alloys with the specified Ni content, and the values lie almost on the mid-points between the values of Pd–Ni and Pd–Rh binary alloys where the $\Delta\mu_H^\circ$ values for Pd–Rh binary alloys are slightly larger than those for Pd–Ni alloys. The $\Delta\mu_H^\circ$ values for high Ni content Pd–Ni–Rh alloys are a little smaller rather than those for Pd–Ni binary alloys. The standard free energy change ΔG_{plat}° for β-hydride formation in Pd–Ni–Rh alloys increases with the Rh content from that of the Pd–Ni binary alloys with constant Ni content. In particular, for low Ni content Pd–Ni–Rh alloys, the rate of increase in the ΔG_{plat}° values with Rh content is almost the same as that for Pd–Rh alloys, where the stability of β-hydride for Pd–Rh binary alloys is slightly greater than that of Pd–Ni alloys.

Keywords: Absorption; Hydrogen; Ternary alloys

1. Introduction

The different solubilities of hydrogen in most palladium-rich Pd binary solid solution alloys, especially at low hydrogen pressure, can be associated mainly with the difference in the elastic strain energy due to the expansion of the Pd lattice for the occupation of octahedral interstices by hydrogen atoms [1–8]; there are some exceptions [9–15] to the lattice "expanded–contracted" classification of Pd alloys as a result of their different hydrogen solubilities.

With respect to the influence of lattice "expansion–contraction" of Pd binary alloys relative to pure Pd, the present authors [16,17] have expanded the scope of such studies by examining the solubility of hydrogen in ternary solid solution alloys of Pd–Cu–Au [16] and Pd–Y–Ag [17]. In the former ternary alloys, a Cu atom contracts the Pd lattice, while an Au atom expands the host lattice. For the latter alloys, both Y and Ag atoms expanded the Pd lattice; however, the lattice expansion caused by Y is much greater than that by Ag.

It has been found that the relative partial molar thermodynamic quantities for solution of hydrogen at infinite dilution and the $\alpha+\beta$ plateau thermodynamic parameters for the Pd–Cu–Au alloys with solute metal atom fraction $X_{Cu}+X_{Au}$ up to 0.2, where $X_{Cu}=X_{Au}$, fall near the mid-points between those of each Pd–Cu and Pd–Au alloy. In the case of Pd–Y–Ag alloys [17] with $X_{Ag}=0.05$ and with X_Y up to 0.063, the thermodynamic parameters for hydrogen solution at infinite dilution and the plateau thermodynamic quantities change from those of Pd–Ag binary alloy with $X_{Ag}=0.05$ with increasing Y content, almost parallel to that found in Pd–Y binary alloys. Therefore, the solubility of hydrogen in these ternary alloys seems to depend mainly

SSDI 0925-8388(94)01353-5

on the magnitude of the strain energy for hydrogen occupation of the octahedral interstices in the alloys, where the compressibility of the alloys also plays part.

In the present investigation, the hydrogen absorption characteristics of Pd-rich Pd–Ni–Rh alloys will be studied, where both substituent metal atoms contract the Pd lattice but the lattice contraction caused by Ni [6,18] is larger than that by Rh [19]. Hydrogen absorption isotherms for Pd–Ni and Pd–Rh binary alloys have been determined by several workers [6,9,20–26]. The trends in the relative chemical potential $\Delta\mu_H^\circ$ for hydrogen solution at infinite dilution and the standard free energy change ΔG_{plat}° for β-hydride formation in both Pd–Ni [6,24] and Pd–Rh [9,20,21,26] alloys correspond to these for "lattice-contracted Pd alloys", i.e. the dissolved hydrogen in the dilute phase region and the β-hydride become increasingly unstable with increasing Ni and Rh contents.

It was recently reported [21] for the pressure–composition isotherms of Pd–Rh binary alloys containing about 7.5 at.% Rh that, in addition to the normal $\alpha+\beta$ two-phase plateau pressures, another "anomalous plateau" was observed near the normal β_{min} phase boundaries. The formation of the anomalous plateau pressures implies that, even in alloys annealed in the usual way, some precursory phase separation together with the metastable and homogeneous solid solutions already exist. The hydrogen solubilities compared at a hydrogen pressure of 1000 Torr exhibit a maximum at about 7.5 at.% Rh.

2. Experimental details

The compositions of Pd–Ni–Rh alloys used in this study were as follows: (1) $Pd_{97.5-x}Ni_{2.5}Rh_x$ with x (at.% Rh) = 0 (Pd–2.5 at.% Ni), 2.5, 5.0, 7.5, (2) $Pd_{95.0-x}Ni_{5.0}Rh_x$ with $x=5.0$, (3) $Pd_{90.0-x}Ni_{10.0}Rh_x$ with $x=7.5$, and (4) $Pd_{87.5-x}Ni_{12.5}Rh_x$ with $x=2.5$, 5.0. They were prepared by arc melting the pure components under argon. The resulting alloy buttons were annealed and rolled into foils about 75 μm thick. Finally, the alloy samples were annealed at 1123 K for 2 h in vacuo and cooled to room temperature at a rate of 300–360 K h^{-1}.

X-ray diffraction studies were carried out at room temperature in order to examine the lattice parameters a_{ss} of hydrogen-free alloys, and also the lattice parameters $a_{\alpha max}$ and $a_{\beta min}$ at the phase boundary compositions within the $\alpha+\beta$ miscibility gaps in hydrogenated alloys. The hydrogenation was carried out electrolytically at 298 ± 1 K. Details of the procedure have been described previously [18,19].

The pressure–composition isotherms for hydrogen absorption were obtained as previously described [6,21]. For the alloy samples of (3) $Pd_{90.0-x}Ni_{10.0}Rh_x$ with $x=7.5$ and (4) $Pd_{87.5-x}Ni_{12.5}Rh_x$ with $x=2.5$, 5.0, desorption isotherms were also measured after the absorption isotherm measurements up to 10 000 Torr.

3. Results and discussion

3.1. X-ray diffraction study

The X-ray diffraction studies confirmed that all the alloys used in this study are single-phase f.c.c. α-Pd, where α-Pd refers to a solid solution of substituted metal in the f.c.c. Pd lattice. Fig. 1 shows the room temperature lattice parameters a_{ss} of the hydrogen-free alloys as a function of the solute metal atom fraction $X_u = X_{Ni} + X_{Rh}$ together with those of the previously determined Pd–Ni [6,18] and Pd–Rh [19] binary alloys. It can be seen that the lattice parameters of the ternary alloys decrease with increasing Rh content from those of Pd–Ni alloys with the specified Ni content, and the rate of decrease with Rh content is almost the same as that for the Pd–Rh binary alloys [19]. Similarly, it can be seen that the lattice parameters of the ternary alloys decrease with Ni content from those of Pd–Rh alloys with a fixed Rh content, and also the decreasing rate is nearly equal to that of Pd–Ni binary alloys. Fig. 2 shows a partial three-dimensional representation of the lattice parameters of the Pd–Ni–Rh ternary alloys [6,18,19]. Table 1 summarizes the lattice parameters of the ternary alloys, together with that of Pd–2.5 at.%

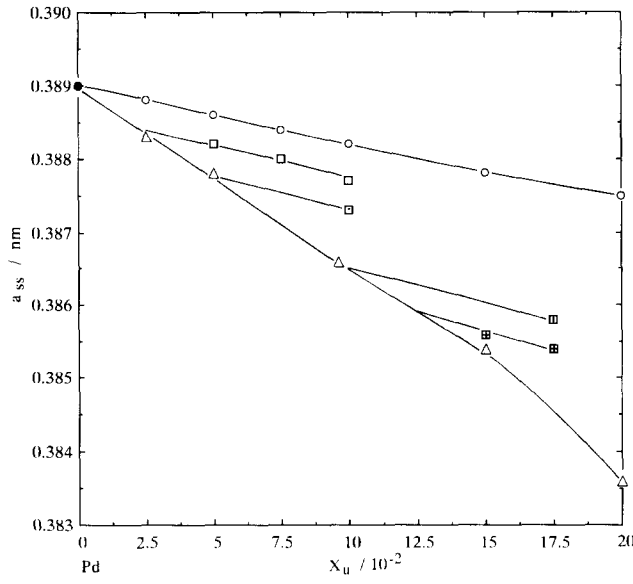

Fig. 1. The room temperature lattice parameters of hydrogen-free Pd–Ni–Rh alloys as a function of the total solute atom fraction $X_u = X_{Ni} + X_{Rh}$ together with those of Pd–Ni and Pd–Rh binary alloys: □, $Pd_{97.5-x}Ni_{2.5}Rh_x$, $x=2.5$, 5.0, 7.5; ⊡, $Pd_{95.0-x}Ni_{5.0}Rh_x$, $x=5.0$; ⊞, $Pd_{90.0-x}Ni_{10}Rh_x$, $x=7.5$; ⊞, $Pd_{87.5-x}Ni_{12.5}Rh_x$, $x=2.5$, 5.0; △, Pd–Ni [6, 18]; ○, Pd–Rh [19].

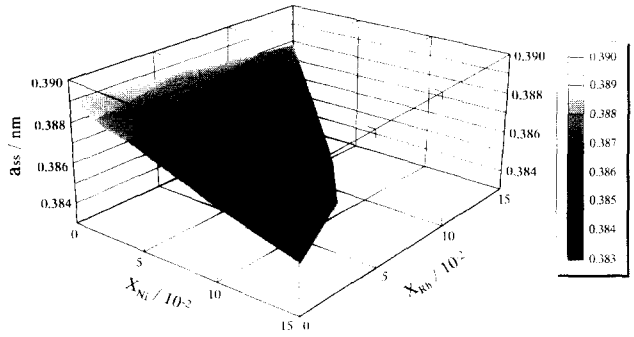

Fig. 2. Partial three-dimensional representation of the lattice parameters of Pd–Ni–Rh alloys [6,18,19].

Table 1
The room temperature lattice parameters a_{ss} of the hydrogen-free f.c.c. Pd-rich Pd–Ni–Rh alloys together with those for the α_{max} and β_{min} phase boundaries in the Pd–Ni–Rh systems

Alloy	$a_{ss} \pm 0.0001$ (nm)	$a_{\alpha max}$ (nm)	$a_{\beta min}$ (nm)
Pd	0.3890	0.3895 ± 0.0001	0.4025 ± 0.0001
$Pd_{97.5-x}Ni_{2.5}Rh_x$			
$x=0$	0.3883	0.3890 ± 0.0001	0.4015 ± 0.0001
$x=2.5$	0.3882	0.3886 ± 0.0001	0.4018 ± 0.0001
$x=5.0$	0.3880	0.3883 ± 0.0001	0.4015 ± 0.0001
$x=7.5$	0.3877	0.3880 ± 0.0001	0.4011 ± 0.0002
$Pd_{95.0-x}Ni_{5.0}Rh_x$			
$x=0$	0.3878	0.3885 ± 0.0001	0.4003 ± 0.0001
$x=5.0$	0.3873	0.3876 ± 0.0001	0.4005 ± 0.0001
$Pd_{90.0-x}Ni_{10}Rh_x$			
$x=7.5$	0.3858	0.3866 ± 0.0001	0.3994 ± 0.0002
$Pd_{87.5-x}Ni_{12.5}Rh_x$			
$x=2.5$	0.3856	0.3863 ± 0.0001	0.3972 ± 0.0002
$x=5.0$	0.3854	0.3860 ± 0.0001	0.3970 ± 0.0002

Ni ($Pd_{97.5-x}Ni_{2.5}Rh_x$: $x=0$) alloy determined newly in this study.

The lattice parameters $a_{\alpha max}$ and $a_{\beta min}$ at the α_{max} and β_{min} phase boundary compositions in hydrogenated ternary alloys are plotted against the solute metal content in Fig. 3, together with those of the Pd–Ni [18] and Pd–Rh [19] binary alloys. These values of $a_{\alpha max}$ and $a_{\beta min}$ are also given in Table 1. The dependence of the $a_{\beta min}$ values on the Rh content in relatively low Ni content Pd–Ni–Rh ternary alloys is a similar behaviour to that of the Pd–Rh binary alloys [19], i.e. an initial increase in the $a_{\beta min}$ value with increasing Rh content. On the contrary, the $a_{\alpha max}$ values decrease slowly with Rh content from those of Pd–Ni alloys with the specified Ni content.

3.2. Pressure–composition–temperature relationships

The pressure–composition isotherms for $Pd_{97.5-x}Ni_{2.5}Rh_x$ alloys with $x=0$, 2.5, 5.0, 7.5 are shown in Figs. 4(a)–4(d) respectively and Fig. 5 shows a comparison of the pressure–composition isotherms at 273 K between the $Pd_{97.5-x}Ni_{2.5}Rh_x$ alloys, together with that of pure Pd [13]. The hydrogen concentration is expressed as $r=[H]/[M]$, i.e. the ratio of the number of hydrogen atoms to the total number of metal atoms. Figs. 6 and 7 show the pressure–composition isotherms for $Pd_{95.0-x}Ni_{5.0}Rh_x$, $x=5.0$, and $Pd_{90.0-x}Ni_{10.0}Rh_x$, $x=7.5$, alloys respectively. The isotherms for $Pd_{87.5-x}Ni_{12.5}Rh_x$ alloys with $x=2.5$, 5.0 are shown in Figs. 8(a) and (b) respectively. Fig. 9 shows the comparison of the absorption isotherms at 303 K between $Pd_{95.0-x}Ni_{5.0}Rh_x$, $x=5.0$, $Pd_{90.0-x}Ni_{10.0}Rh_x$, $x=7.5$, and $Pd_{87.5-x}Ni_{12.5}Rh_x$, $x=2.5$, 5.0, alloys. The desorption isotherms shown in Figs. 7 and 8 are incomplete because the desorption kinetics were very sluggish.

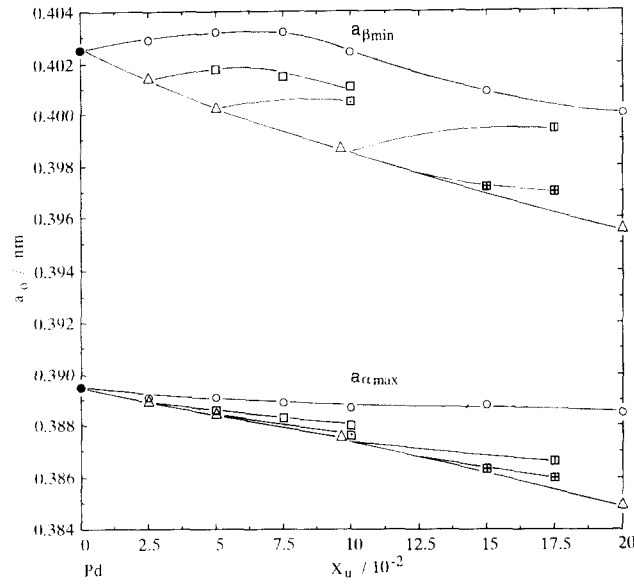

Fig. 3. The room temperature lattice parameters $a_{\alpha max}$ and $a_{\beta min}$ at the α_{max} and β_{min} phase boundary compositions in hydrogenated Pd–Ni–Rh alloys as a function of $X_u = X_{Ni} + X_{Rh}$, together with those of hydrogenated Pd–Ni and Pd–Rh binary alloys: □, $Pd_{97.5-x}Ni_{2.5}Rh_x$, $x=2.5$, 5.0, 7.5; ⊡, $Pd_{95.0-x}Ni_{5.0}Rh_x$, $x=5.0$; ◫, $Pd_{90.0-x}Ni_{10}Rh_x$, $x=7.5$; ⊞, $Pd_{87.5-x}Ni_{12.5}Rh_x$, $x=2.5$, 5.0; △, Pd–Ni [18]; ○, Pd–Rh [19].

It can be seen that the low pressure solubilities in Pd–Ni–Rh alloys at a given temperature decrease with increasing Ni and Rh content, and the $\alpha+\beta$ plateau pressures p_{plat} increase. The high pressure solubilities in the ternary alloys decrease with increasing Ni content but increase with Rh content. The hydrogen capacities at $p_{H_2}=1000$ Torr and at a given temperature in the Pd–Ni–Rh alloys with a given Ni content exhibit a maximum around 7.5 at.% Rh, just as do Pd–Rh binary alloys. The trend in the hydrogen capacities for the ternary alloys corresponds to the variation in the lattice expansion at the β_{min} phase boundaries as shown in Fig. 3.

In the previous study of Pd–Rh binary alloy–H systems [21], especially for the isotherms of Pd–

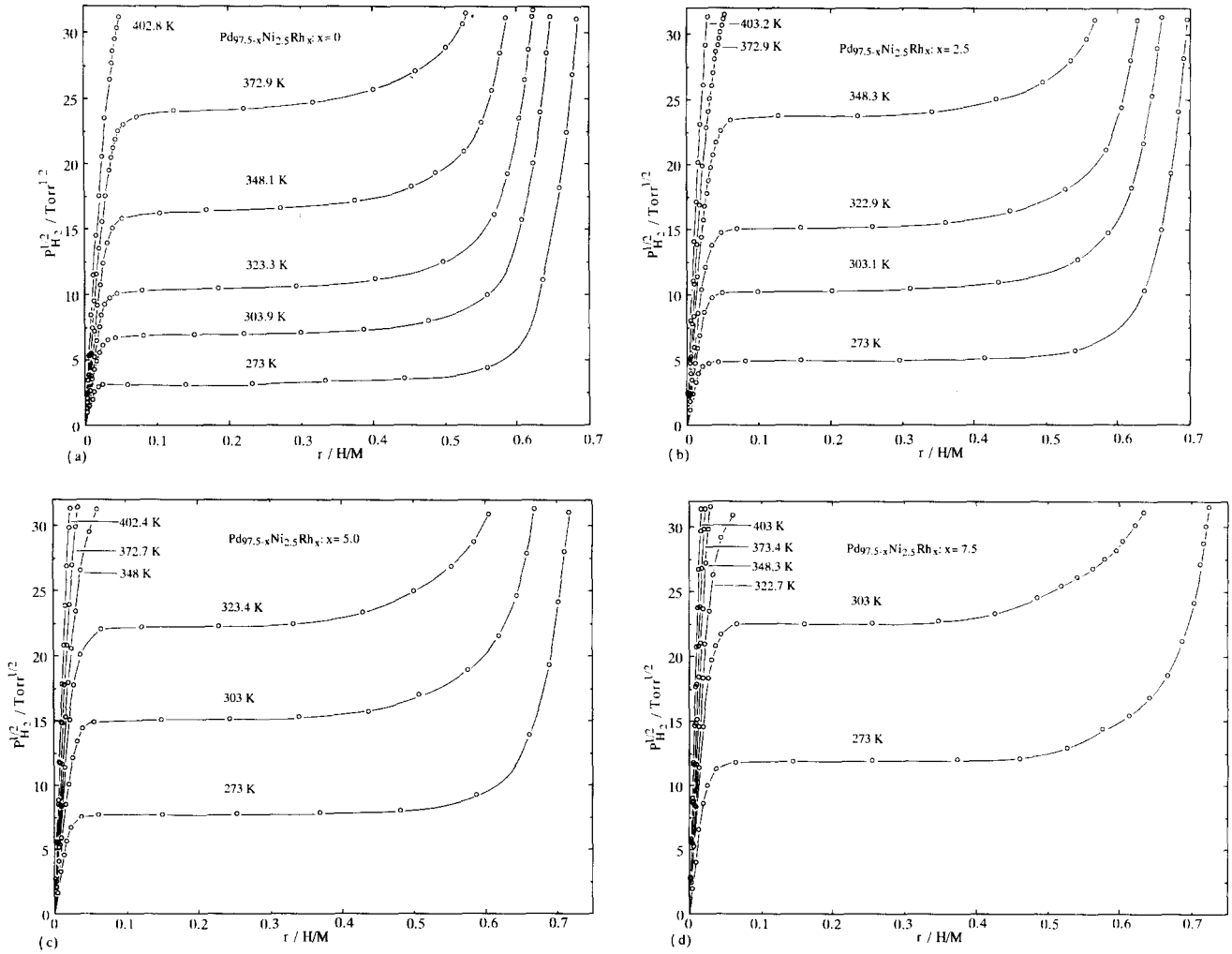

Fig. 4. Pressure–composition isotherms for hydrogen absorption for $Pd_{97.5-x}Ni_{2.5}Rh_x$ alloys: (a) $x=0$; (b) $x=2.5$; (c) $x=5.0$; (d) $x=7.5$.

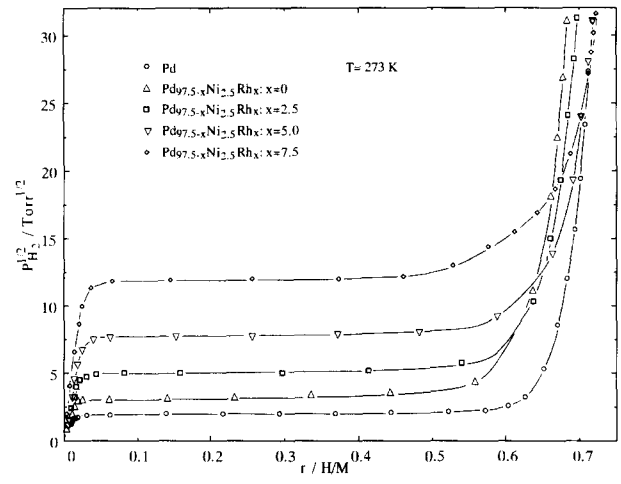

Fig. 5. A comparison of the pressure–composition isotherms at 273 K between $Pd_{97.5-x}Ni_{2.5}Rh_x$ alloy with $x=0$, 2.5, 5.0 and 7.5 and pure Pd.

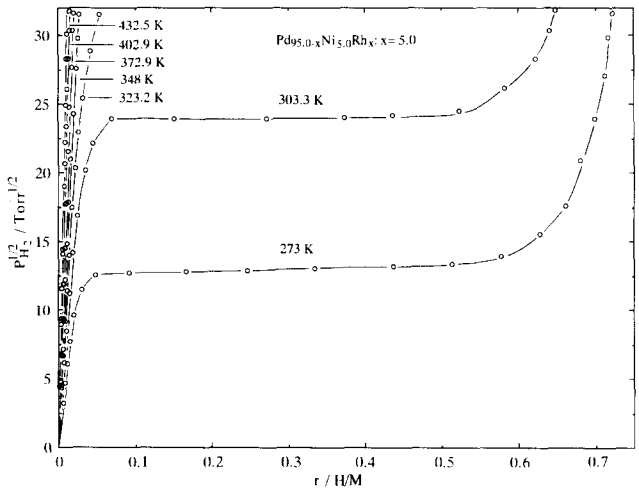

Fig. 6. Pressure–composition isotherms for hydrogen absorption by the $Pd_{95.0-x}Ni_{5.0}Rh_x$ alloy with $x=5.0$.

7.5 at.% Rh alloy, anomalous plateau pressures have been observed near the normal β_{min} composition, but in the present Pd–Ni–Rh alloys such anomalous plateau pressures have not been clearly observed; this may be due to the effect of Ni addition in the alloys.

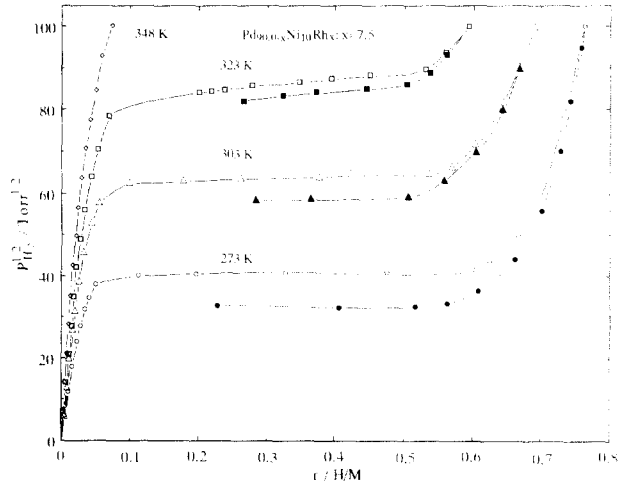

Fig. 7. Pressure–composition isotherms for hydrogen absorption and desorption by the $Pd_{90.0-x}Ni_{10}Rh_x$ alloy with $x=7.5$. The desorption isotherms are shown by the full-symbols.

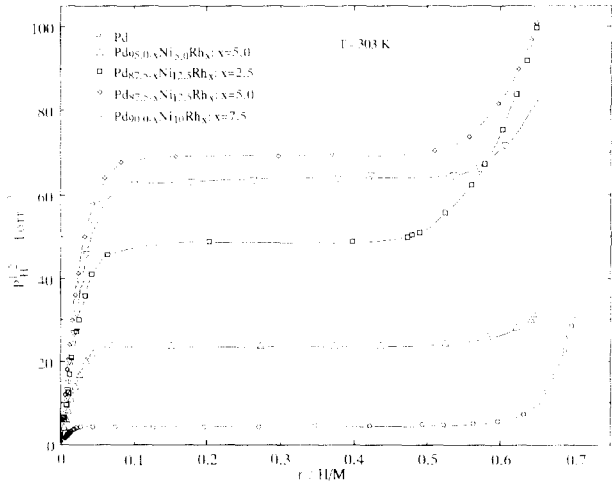

Fig. 9. A comparison of the absorption pressure–composition isotherms at 303 K between the $Pd_{95.0-x}Ni_{5.0}Rh_x$, $x=5.0$, $Pd_{90.0-x}Ni_{10}Rh_x$, $x=7.5$, and $Pd_{87.5-x}Ni_{12.5}Rh_x$, $x=2.5$, 5.0, alloys and pure Pd.

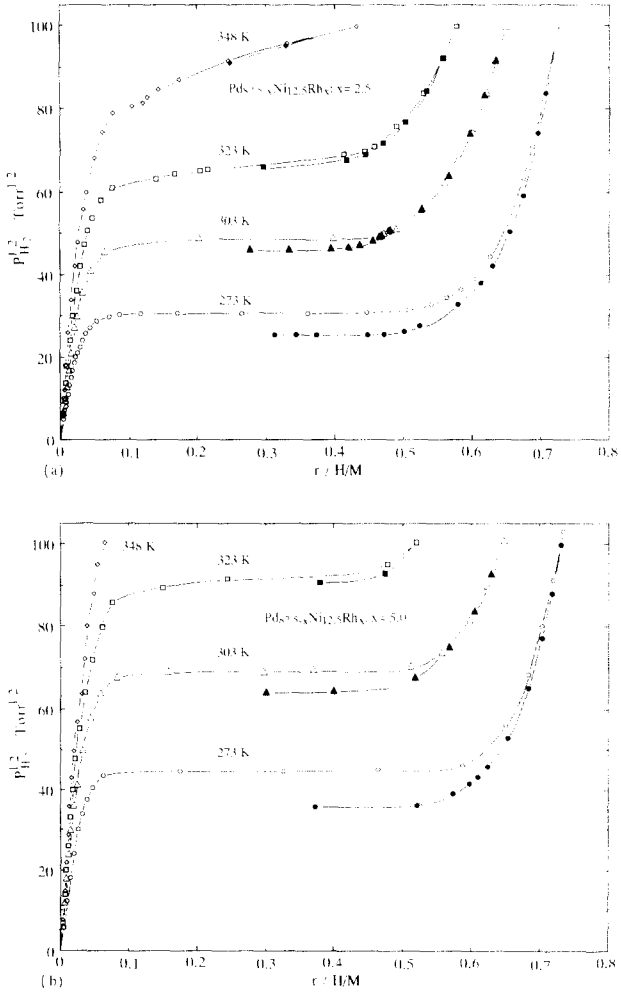

Fig. 8. Pressure–composition isotherms for hydrogen absorption and desorption by $Pd_{87.5-x}Ni_{12.5}Rh_x$ alloys with $x=$(a) 2.5 and (b) 5.0. The desorption isotherms are shown by the full symbols.

3.3. Thermodynamic parameters of hydrogen solution in the dilute phase region

The relative chemical potential $\Delta\mu_H^\circ$ of dissolved hydrogen at infinite dilution in Pd–Ni–Rh alloys was obtained from the relation $RT \ln p_{H_2}^{1/2} (1-r/\beta)/(r/\beta) = \Delta\mu_H^\circ + g_1 r/\beta$, where β is the number of octahedral sites per lattice atom and was taken as unity [13]. g_1 is the apparent H–H pair interaction free energy between dissolved hydrogen, and $g_1 r$ is an approximation to the excess chemical potential $\mu_H^E(r)$.

The relative partial molar enthalpy ΔH_H° and entropy ΔS_H° of solution of hydrogen at infinite dilution were determined from the temperature dependence of $\Delta\mu_H^\circ$ values. Fig. 10 shows plots of $\Delta\mu_H^\circ$ at 298 K against atom fraction $X_u = X_{Ni} + X_{Rh}$ for the ternary alloys, in comparison with the previously determined data for the Pd–Ni [6,24] and Pd–Rh [20,21,24] binary alloys. Figs. 11 and 12 show plots of ΔH_H° and ΔS_H° respectively against X_u in the ternary alloys in comparison with those of the Pd–Ni [6,24] and Pd–Rh [20,21,24] binary alloys. These values of ΔH_H°, ΔS_H° and g_1 at 348 K are summarized in Table 2.

It can be seen from Fig. 10 that the dissolved hydrogen in the dilute phase region in the Pd–Ni–Rh alloys becomes more unstable with increase in solute metal content X_u. The $\Delta\mu_H^\circ$ values for $Pd_{97.5-x}Ni_{2.5}Rh_x$ alloys with $x=2.5$, 5.0 and 7.5 increase with Rh content from that for Pd–2.5 at.% Ni alloy and have a tendency to lie almost at the mid-points between the $\Delta\mu_H^\circ$ values for the Pd–Ni and Pd–Rh binary alloys, where the dissolved hydrogen in Pd–Rh binary alloys is slightly less stable compared with that in Pd–Ni alloys over comparable alloy compositions. The $\Delta\mu_H^\circ$ value for $Pd_{95.0-x}Ni_{5.0}Rh_x$ with $x=5.0$ is almost the same as that of the Pd–10 at.% Ni alloy, and the values for high

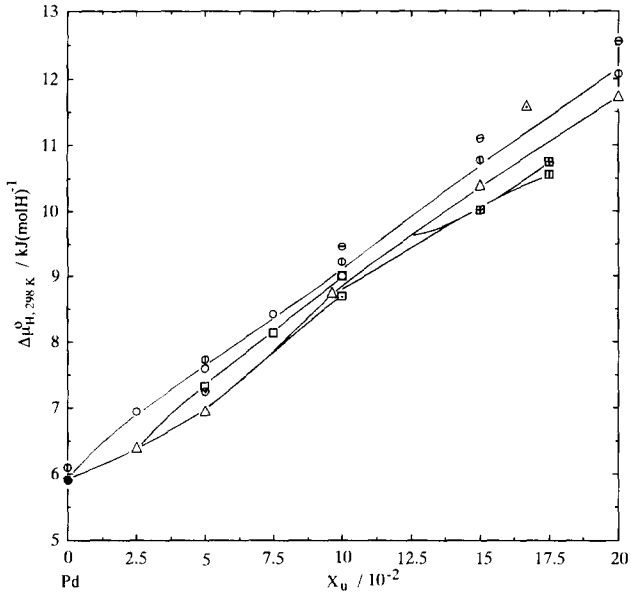

Fig. 10. Plots of $\Delta\mu^{\circ}_{H}$ at 298 K vs. X_u for Pd–Ni–Rh ternary alloys together with those for Pd–Ni and Pd–Rh binary alloys: □, $Pd_{97.5-x}Ni_{2.5}Rh_x$, $x=2.5$, 5.0, 7.5; ⊡, $Pd_{95.0-x}Ni_{5.0}Rh_x$, $x=5.0$; ⊞, $Pd_{90.0-x}Ni_{10}Rh_x$, $x=7.5$; ⊞, $Pd_{87.5-x}Ni_{12.5}Rh_x$, $x=2.5$, 5.0; △, Pd–Ni [6]; ▲, Pd–Ni [24]; ○, Pd–Rh [21]; ⊕, Pd–Rh [20], slowly quenched; ⊖, Pd–Rh [20], rapidly quenched; ⊙, Pd–Rh [24].

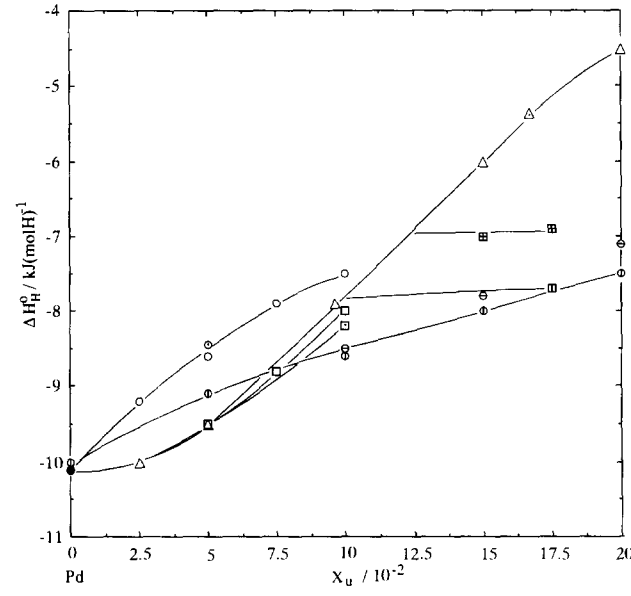

Fig. 11. Plots of ΔH°_{H} vs. X_u for Pd–Ni–Rh ternary alloys together with those for Pd–Ni and Pd–Rh binary alloys: □, $Pd_{97.5-x}Ni_{2.5}Rh_x$, $x=2.5$, 5.0, 7.5; ⊡, $Pd_{95.0-x}Ni_{5.0}Rh_x$, $x=5.0$; ⊞, $Pd_{90.0-x}Ni_{10}Rh_x$, $x=7.5$; ⊞, $Pd_{87.5-x}Ni_{12.5}Rh_x$, $x=2.5$, 5.0; △, Pd–Ni [6]; ▲, Pd–Ni [24]; ○, Pd–Rh [21]; ⊕, Pd–Rh [20], slowly quenched; ⊖, Pd–Rh [20], rapidly quenched; ⊙, Pd–Rh [24].

Ni content Pd–Ni–Rh alloys such as $Pd_{90.0-x}Ni_{10.0}Rh_x$ with $x=7.5$ and $Pd_{87.5-x}Ni_{12.5}Rh_x$ with $x=2.5$, 5.0 are somewhat smaller than those in Pd–Ni binary alloys with $X_u=X_{Ni}$. The apparent H–H attractive interaction energies g_1 in the ternary alloys (Table 2) have a tendency to decrease with increasing X_{Ni} and X_{Rh}, as in Pd–Rh binary alloys.

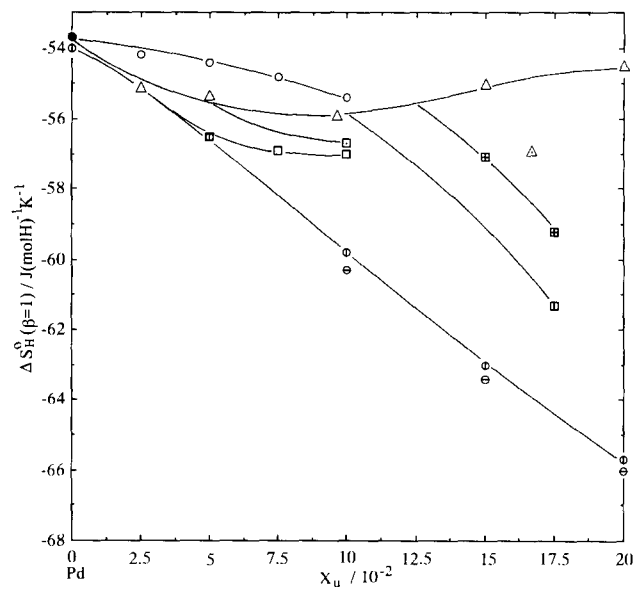

Fig. 12. Plots of $\Delta S^{\circ}_{H}(\beta=1)$ vs. X_u for Pd–Ni–Rh ternary alloys together with those for Pd–Ni and Pd–Rh binary alloys: □, $Pd_{97.5-x}Ni_{2.5}Rh_x$, $x=2.5$, 5.0, 7.5; ⊡, $Pd_{95.0-x}Ni_{5.0}Rh_x$, $x=5.0$; ⊞, $Pd_{90.0-x}Ni_{10}Rh_x$, $x=7.5$; ⊞, $Pd_{87.5-x}Ni_{12.5}Rh_x$, $x=2.5$, 5.0; △, Pd–Ni [6]; ▲, Pd–Ni [24]; ○, Pd–Rh [21]; ⊕, Pd–Rh [20], slowly quenched; ⊖, Pd–Rh [20], rapidly quenched.

The values of ΔH°_{H} for Pd–Ni–Rh alloys become less exothermic with increasing solute metal content, and the values for low Ni content ternary alloys are close to those for Pd–Ni binary alloys at the same solute content. The values for high Ni content ternary alloys tend toward those of the Pd–Rh binary alloys with the corresponding solute metal content. The ΔH°_{H} values for Pd–Ni binary alloys with less than about 7.5 to 10 at.% Ni are a little more exothermic than those for Pd–Rh binary alloys, despite the larger lattice contraction for the Pd–Ni alloys. However, the enthalpy values for high Ni content Pd–Ni binary alloys are less exothermic than those of the Pd–Rh binary alloys. Judging from the bulk modulus of Ni and Rh [27], the greater exothermicity of the ΔH°_{H} values for Pd–Ni binary alloys containing relatively low Ni content may be due to a decrease in the strain energy required to expand the lattice to accommodate hydrogen atoms because of the larger compressibility of Pd–Ni alloys compared with Pd–Rh alloys which more than counterbalances the effect of the smaller size of the octahedral interstices in Pd–Ni alloys.

It can be seen from Fig. 12 that the values of $\Delta S^{\circ}_{H}(\beta=1)$ in Pd–Ni–Rh ternary alloys decrease with Rh content from those of the Pd–Ni binary alloys with the specified Ni content and, in the case of low Ni content Pd–Ni–Rh alloys with less than 5.0 at.% Ni, the decrease rate is similar to that of Pd–Rh binary alloys with less than 10 at.% Rh [21]. On the contrary, for the case of high Ni content ternary alloys with 10.0 and 12.5 at.% Ni, the decrease in rate is almost the

Table 2
Thermodynamic parameters for hydrogen absorption by Pd–Ni–Rh alloys

Alloy	ΔH_H° (kJ (mol H)$^{-1}$)	ΔS_H° (J (mol H)$^{-1}$ K^{-1})	g_1 [a] (kJ (mol H)$^{-1}$)	ΔH_{plat}° (kJ (mol H)$^{-1}$)	ΔS_{plat}° (J (mol H)$^{-1}$ K^{-1})	ΔH_{solv}^z (kJ (mol H)$^{-1}$)	ΔS_{solv}^z (J (mol H)$^{-1}$ K^{-1})
Pd	−10.1	−53.7	−47.3	−18.4	−45.5	10.7	2.3
$Pd_{97.5-x}Ni_{2.5}Rh_x$							
$x=0$	−10.0	−55.1	−39.5	−17.3	−45.1	8.5	−2.0
$x=2.5$	−9.5	−56.5	−40.8	−16.3	−45.5	7.6	−4.1
$x=5.0$	−8.8	−56.9	−41.7	−15.3	−45.5	5.1	−10.2
$x=7.5$	−8.0	−57.0	−44.6	−14.4	−45.9	4.1	−13.1
$Pd_{95.0-x}Ni_{5.0}Rh_x$							
$x=5.0$	−8.2	−56.7	−32.9	−14.2	−45.7	6.7	−1.3
$Pd_{90.0-x}Ni_{10}Rh_x$							
$x=7.5$	−7.7	−61.3	−35.6	−10.7	−42.2	7.3	1.6
$Pd_{87.5-x}Ni_{12.5}Rh_x$							
$x=2.5$	−7.0	−57.1	−35.3	−11.2	−42.0	6.9	−0.8
$x=5.0$	−6.9	−59.2	−35.5	−10.5	−42.2	7.9	3.3

[a] $T=348$ K and $\beta=1$.

same as that of high Rh content Pd–Rh binary alloys [20].

Clewley et al. [9] and the present authors [6] have previously found that Pd–Rh and Pd–Ni alloys have similar insensitivities of $\Delta S_H^\circ(\beta=1)$ values to Rh and Ni contents of the alloys, just as has been recently observed for Pd–Cu alloys [16]. Pd–Rh, Pd–Ni and Pd–Cu alloys exhibit similar behaviours in regard to ΔS_H° which differ from those of other substituent metals. In their pure state these metals form monohydride phases and the former two solute metal hydrides are isomorphous f.c.c. with β-Pd hydride and the latter solute metal hydride is a hexagonal wurtzite structure. Thus, the relative insensitivity of $\Delta S_H^\circ(\beta=1)$ values to the solute metal content in Pd alloys where all the octahedral sites are equally accessible to hydrogen may depend on whether or not there is monohydride formation of pure solute metals. However, this is not necessarily the case, because the present authors [14,15] have recently found that for Pd–Li solid solution alloys there is regularly a significant decrease in the relative partial excess entropy of solution of hydrogen with increasing Li content and because the hydride phase which the substituent metal, Li, in its pure state forms is isomorphous with β-Pd hydride. LiH is, however, an ionic solid and the others are metallic.

3.4. The $\alpha+\beta$ plateau thermodynamic parameters

From the plateau pressure corresponding to the $\alpha+\beta$ two-phase region in Pd–Ni–Rh alloys, the standard enthalpy change ΔH_{plat}° and entropy ΔS_{plat}° for β-hydride formation were obtained from the relation $\Delta G_{plat}^\circ = RT \ln p_{plat}^{1/2} = \Delta H_{plat}^\circ - T\,\Delta S_{plat}^\circ$.

The thermodynamic parameters for the hydrogen solvus were evaluated from plots of $-R \ln a/(1-a)$ vs. T^{-1}, where a is the solvus composition [13]. The derived thermodynamic parameters are given in Table 2, where ΔH_{solv}^z and ΔS_{solv}^z are the standard enthalpy and entropy changes respectively for solvus formation.

Fig. 13 shows plots of the standard free energy change ΔG_{plat}° at 298 K for β-hydride formation in Pd–Ni–Rh alloys against the solute metal content in comparison with those in previously determined data for the Pd–Ni [6] and Pd–Rh [20,21] binary alloys. The stability of the β-hydride decreases with increase in X_u, where u = Ni or Rh or Ni + Rh. The stability of the Pd–Rh binary alloys is slightly greater than the stability of the Pd–Ni binary alloys, although, as shown in Fig. 10, hydrogen in the dilute phase region of Pd–Ni alloys is more stable than in Pd–Rh alloys.

It is of interest that the ΔG_{plat}° values of Pd–Ni–Rh alloys increase with Rh content from the values of the Pd–Ni binary alloys with a given Ni content. In particular, for low Ni content Pd–Ni–Rh alloys the rate of increase in ΔG_{plat}° with Rh content is almost the same as for

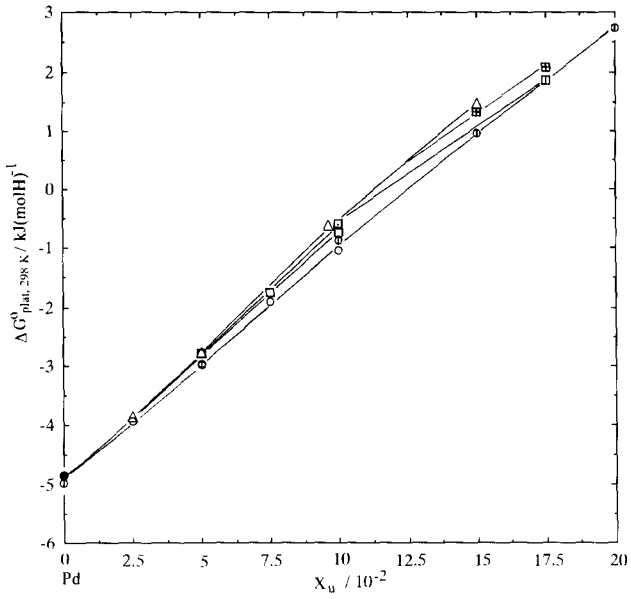

Fig. 13. Plots of ΔG°_{plat} at 298 K vs. X_u for Pd–Ni–Rh ternary alloys together with those for Pd–Ni and Pd–Rh binary alloys: □, $Pd_{97.5-x}Ni_{2.5}Rh_x$, $x=2.5$, 5.0, 7.5; ⊡, $Pd_{95.0-x}Ni_{5.0}Rh_x$, $x=5.0$; ⊞, $Pd_{90.0-x}Ni_{10}Rh_x$, $x=7.5$; ⊞, $Pd_{87.5-x}Ni_{12.5}Rh_x$, $x=2.5$, 5.0; △, Pd–Ni [6]; ○, Pd–Rh [21]; ⊙, Pd–Rh [20], slowly quenched.

Pd–Rh alloys [20,21]. Thus, as can be seen from the variations in the lattice parameters of hydrogen-free alloys (Fig. 1), the stability of β-hydride in Pd–Ni–Rh ternary alloys is mainly associated with the lattice "expanded–contracted" effect of Pd alloys.

Values of ΔG^{z}_{solv} at 298 K in the ternary alloys decrease more or less with increasing solute metal content. The solid solubility limit of hydrogen, i.e. α_{max} composition in the ternary alloy–hydrogen systems increases with the solute metal content. Compared with the ΔG^{z}_{solv} values of Pd–Ni [6] binary alloys, values of the present Pd–Ni–Rh ternary alloys and Pd–Rh [21] binary alloys are slightly larger. The trend in ΔG^{z}_{solv} values at 298 K with the solute metal content is similar to the results shown in Fig. 3 for the lattice expansion at the α_{max} compositions determined by X-ray diffraction.

4. Conclusions

(1) The room temperature lattice parameters of hydrogen-free Pd–Ni–Rh ternary alloys decrease with increasing Rh content from those of Pd–Ni binary alloys with a specified Ni content, and the rate of decrease is almost the same as for Pd–Rh binary alloys. The dependence of Rh content on the lattice parameters at the β_{min} phase boundary compositions in low Ni content Pd–Ni–Rh alloys appears to behave similarly to that of hydrogenated Pd–Rh binary alloys, which exhibit an increase in the $a_{\beta min}$ value with Rh content up to about 7.5 at.%. In contrast, the $a_{\alpha max}$ values in the ternary alloys decrease slowly with increasing Rh content from those of Pd–Ni binary alloys with the specified Ni content.

(2) The low pressure solubilities in Pd–Ni–Rh alloys decrease with increasing Ni and Rh contents, and the $\alpha+\beta$ plateau pressures increase. The high pressure solubilities decrease with increasing Ni content, whereas they increase with Rh content. The hydrogen capacities in the ternary alloys with a given Ni content exhibit a maximum around 7.5 at.% Rh just as in Pd–Rh binary alloys.

(3) The relative chemical potential $\Delta\mu^{\circ}_{H}$ of dissolved hydrogen at infinite dilution in the ternary alloys increases with Rh content from those of Pd–Ni binary alloys with a fixed Ni content, and the values lie almost on the mid-points between the values for Pd–Ni and Pd–Rh binary alloys where the dissolved hydrogen in Pd–Rh binary alloy is slightly less stable compared with that in Pd–Ni binary alloys over the alloy compositions. The $\Delta\mu^{\circ}_{H}$ values for high Ni content Pd–Ni–Rh alloys are, however, a little smaller than those for Pd–Ni alloys.

(4) The standard free energy change ΔG°_{plat} for β-hydride formation in Pd–Ni–Rh alloys increases with Rh content from those of Pd–Ni binary alloys with a fixed Ni content. For low Ni content Pd–Ni–Rh alloys, especially, the rate of increase in the ΔG°_{plat} values with Rh content is almost the same as that of Pd–Rh alloys, where the stability of the β-hydride of Pd–Rh alloys is slightly larger than that of Pd–Ni alloys. The standard change ΔG^{z}_{solv} at 298 K for hydrogen solvus formation, i.e. for α_{max} phase boundary formation in Pd–Ni–Rh alloys, decreases with increasing Ni and Rh content. The hydrogen solubility limits in the α phase for Pd–Ni–Rh and Pd–Rh alloys are a little smaller than those in Pd–Ni alloys.

References

[1] F.A. Lewis, *The Palladium–Hydrogen System*, Academic Press, New York, 1967.
[2] E. Wicke, H. Brodowsky and H. Züchner, in G. Alefeld and J. Völkl (eds.), Hydrogen in Metals II, Springer, Berlin, 1978, *Top. Appl. Phys., 29* (1978) 73.
[3] W.A. Oates and T.B. Flanagan, *Progress in Solid State Chemistry*, Vol. 13, Pergamon, Oxford, 1981, p. 193.
[4] R. Burch and N. Mason, *J. Chem. Soc., Faraday Trans. I, 76* (1980) 2285.
[5] S. Ramaprabhu, R. Leiberich and A. Weiss, *Z. Phys. Chem., N.F., 161* (1989) 83.
[6] Y. Sakamoto, T. Matsuo, H. Sakai and T.B. Flanagan, *Z. Phys. Chem., N.F., 162* (1989) 83.
[7] Y. Sakamoto, K. Kajihara, E. Ono, K. Baba and T. B. Flanagan, *Z. Phys. Chem., N.F., 165* (1989) 67.
[8] F.L. Chen, Y. Sakamoto and T.B. Flanagan, *Ber. Bunsenges. Phys. Chem., 97* (1993) 784.

[9] J.D. Clewley, J.F. Lynch and T.B. Flanagan, *J. Chem. Soc., Faraday Trans. I, 73* (1977) 494.
[10] A. Maeland and T.B. Flanagan, *J. Phys. Chem., 68* (1964) 1419.
[11] Y. Sakamoto, K. Kajihara, T. Kikumura and T.B. Flanagan, *J. Chem. Soc., Faraday Trans., 86* (1990) 377.
[12] K. Kandasamy, F.A. Lewis, W.D. McFall and R.-A. McNicholl, *Z. Phys. Chem., N.F., 163* (1989) 41.
[13] Y. Sakamoto, U. Miyagawa, E. Hamamoto, F.L. Chen, R.-A. McNicholl and T.B. Flanagan, *Ber. Bunsenges. Phys. Chem., 94* (1990) 1457.
[14] Y. Sakamoto, F.L. Chen, J. Muto and T.B. Flanagan, *Z. Phys. Chem., 173* (1991) 235.
[15] Y. Sakamoto, T. Hisamoto, M. Ura, R. Nakamura and T.B. Flanagan, *J. Alloys Comp., 200* (1993) 141.
[16] Y. Sakamoto, N. Ishimaru and Y. Mukai, *Ber. Bunsenges. Phys. Chem., 95* (1991) 680.
[17] Y. Sakamoto, N. Ishimaru and Y. Inoue, *Ber. Bunsenges. Phys. Chem., 96* (1992) 128.
[18] Y. Sakamoto, K. Yuwasa and K. Hirayama, *J. Less-Common Met., 88* (1982) 115.
[19] Y. Sakamoto, K. Baba and T.B. Flanagan, *Z. Phys. Chem., N.F., 158* (1988) 223.
[20] H. Noh, W. Luo and T.B. Flanagan, *J. Alloys Comp., 196* (1993) 7.
[21] Y. Sakamoto, Y. Haraguchi, M. Ura and F.L. Chen, *Ber. Bunsenges. Phys. Chem., 98* (1994) 964.
[22] J.C. Barton, J.A.S. Green and F.A. Lewis, *Trans. Faraday Soc., 62* (1966) 960.
[23] J.A.S. Green and F.A. Lewis, *Trans. Faraday Soc., 62* (1966) 971.
[24] H. Brodowsky and H. Husemann, *Ber. Bunsenges. Phys. Chem., 70* (1966) 626.
[25] B. Baranowski, S. Majchrzak and T.B. Flanagan, *J. Phys. Chem., 77* (1973) 35.
[26] S. Kishimoto, W.A. Oates and T.B. Flanagan, *J. Less-Common Met., 88* (1982) 459.
[27] T. Górecki, *Mater. Sci. Eng., 43* (1980) 225.